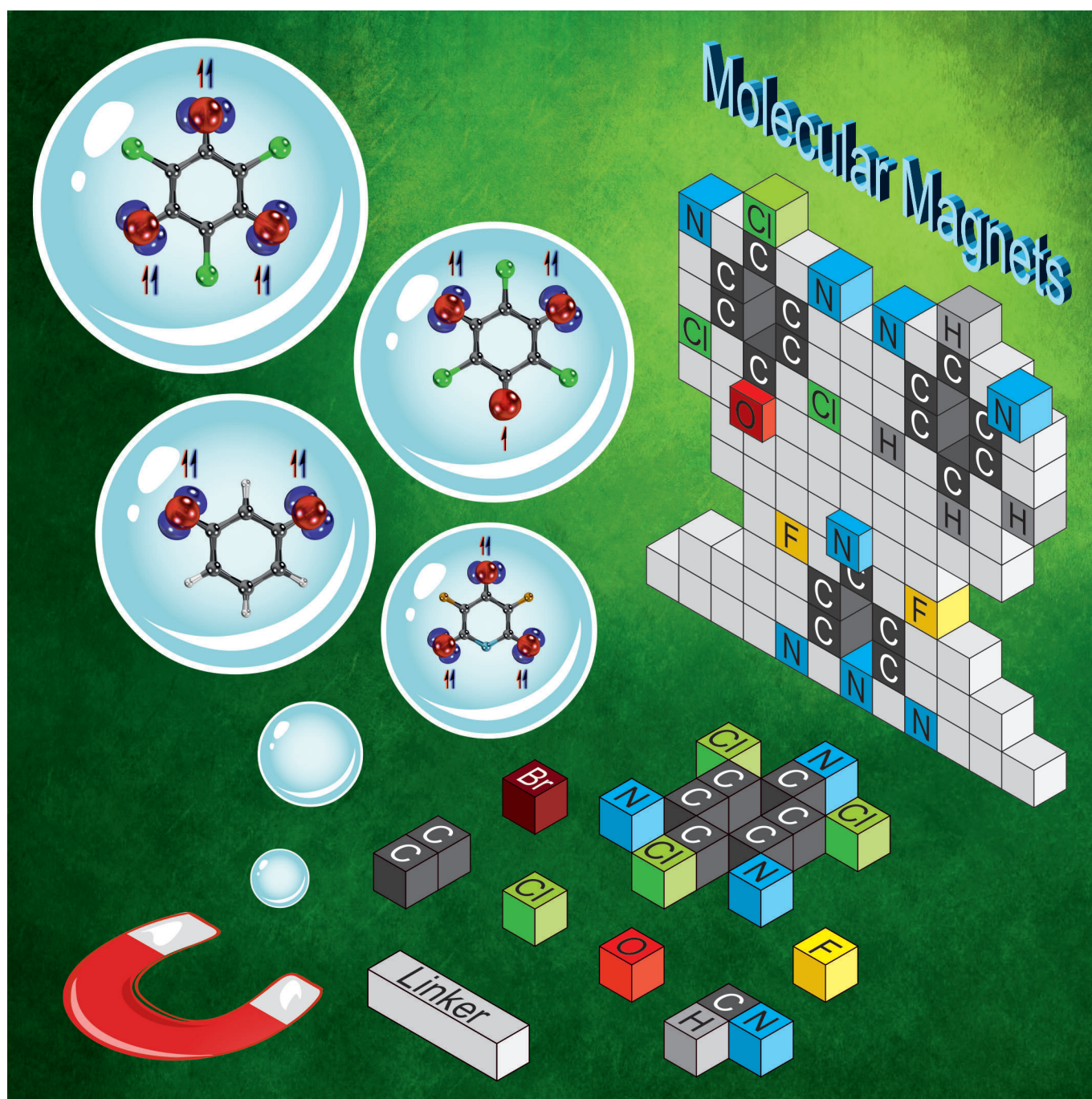


## ■ Magnetism

## Molecular Magnets: The Synthesis and Characterization of High-Spin Nitrenes

Sergei V. Chapyshev,<sup>\*,[a]</sup> Enrique Mendez-Vega,<sup>[b]</sup> and Wolfram Sander<sup>\*,[b]</sup>

**Abstract:** Among all C-, N-, and O-centered polyradicals, high-spin nitrenes possess the largest magnetic anisotropy and are of considerable interest as multi-level molecular spin systems for exploration of organic molecular magnetism and quantum information processing. Although the first representatives of quintet and septet nitrenes were obtained almost 50 years ago, the experimental and theoretical studies of these highly reactive species became possible only re-

cently, owing to new achievements in molecular spectroscopy and computational chemistry. Meanwhile, dozens of various quintet dinitrenes and septet trinitrenes were successfully characterized by IR, UV/Vis, and EPR spectroscopy, thus providing important information about the electronic structure, magnetic properties and reactivity of these compounds.

## 1. Introduction

Nitrenes are neutral reactive species containing a monovalent nitrogen atom with four nonbonding electrons that occupy the valence orbitals resulting in several electronic configurations: triplet ( $S=1$ ), open-shell singlet ( $S=0$ ), and closed-shell singlet ( $S=0$ ).<sup>[1–4]</sup> When aromatic molecules contain two or three nitrene units, unpaired electrons may ferromagnetically (FM) interact to each other, resulting in quintet ( $S=2$ ) or septet ( $S=3$ ) spin states.<sup>[5–8]</sup> Most aryl nitrenes exhibit robust ground triplet states with singlet–triplet energy splittings of about 15–20 kcal mol<sup>-1</sup> due to strong FM exchange interactions between the unpaired electrons (Figure 1).<sup>[9]</sup>

Strong evidence of the ground triplet state of aryl nitrenes was obtained in 1962, when electron paramagnetic resonance (EPR) spectra of several triplet nitrenes formed by photolysis of azides in organic glasses were recorded.<sup>[10]</sup> A few years later, EPR spectral detection of quintet dinitrene **1**<sup>[11]</sup> and septet trinitrene **2**<sup>[12]</sup> was reported. However, the zero-field splitting (ZFS)  $D$  and  $E$  parameters of these nitrenes could not be derived from the experimental EPR spectra.

The preparation of quintet dinitrene **1** stimulated extensive EPR studies of various dinitrenes. These studies were focused on investigations of exchange interactions between the nitrene units, depending on the structure of the linkers.<sup>[6]</sup> It was found that all aromatic dinitrenes can be classified in three main categories: nondisjoint, disjoint, and quinonoidal.<sup>[5,6]</sup> Nondisjoint dinitrenes, for example, **3–8** (Figure 2), have quintet spin states as ground states since their spin polarized  $\pi$ -systems are divided into alternating sites of  $\alpha$  ( $\uparrow$ ) and  $\beta$  ( $\downarrow$ ) spin density (counted as  $n^*$  and  $n^0$ , respectively) with  $n^* > n^0$ . In contrast, disjoint

dinitrenes such as **9–14**, have ground singlet spin states with equal numbers of  $n^*$  and  $n^0$ . For most of these dinitrenes, excited triplet and quintet spin states lie just 100–600 cal mol<sup>-1</sup> above the singlet states. These excited states are observable in the EPR spectra, showing the expected nonlinear thermal Curie law behavior.<sup>[5]</sup>

Quinonoidal dinitrenes, for example, **15–19**, possess ground open-shell singlet spin states, albeit the EPR-active triplet biradicals can be populated at higher temperatures. The electronic structures of these dinitrenes result from pairing of the electrons occupying the out-of-plane  $p_x$  orbitals on the nitrene units.<sup>[5,6]</sup>

Since 1996 the development of advanced programs for EPR spectrum simulations<sup>[13]</sup> opened up new opportunities in investigations of high-spin nitrenes (Figure 3). Hence, the  $D$  and  $E$  values of quintet dinitrenes **20–23** and septet trinitrenes **24** and **25** isolated in organic glasses at cryogenic temperatures have been determined.<sup>[14–18]</sup> These studies showed that high-spin nitrenes possess the largest  $D$  values among all organic polyradicals and thus are promising molecular systems for the design of organic magnetics and multi-level molecular spin systems. However, the most considerable progress in investigations of quintet and septet nitrenes has been achieved in the last 15 years owing to the use of high-frequency W-band EPR spectroscopy<sup>[19]</sup> and EPR spectrometers equipped with spectroscopic cells for the isolation of nitrenes in solid–gas matrices.<sup>[20]</sup> The development of modern computational methods enabled

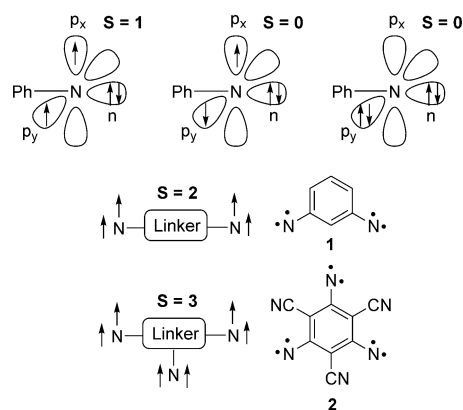


**Figure 1.** Visual depictions of triplet, open- and closed-shell singlet state nitrenes as well as examples of ferromagnetically coupled di- and trinitrenes **1** and **2**.

[a] Dr. S. V. Chapyshev  
 Institute of Problems of Chemical Physics, Russian Academy of Sciences  
 142432 Chernogolovka, Moscow Region (Russia)  
 E-mail: chap@icp.ac.ru

[b] Dr. E. Mendez-Vega, Prof. Dr. W. Sander  
 Lehrstuhl für Organische Chemie II  
 Ruhr-Universität Bochum, 44780 Bochum (Germany)  
 E-mail: wolfram.sander@rub.de

The ORCID identification number(s) for the author(s) of this article can be found under: <https://doi.org/10.1002/chem.202002234>.

© 2020 The Authors. Published by Wiley-VCH GmbH. This is an open access article under the terms of Creative Commons Attribution NonCommercial-NoDerivs License, which permits use and distribution in any medium, provided the original work is properly cited, the use is non-commercial and no modifications or adaptations are made.

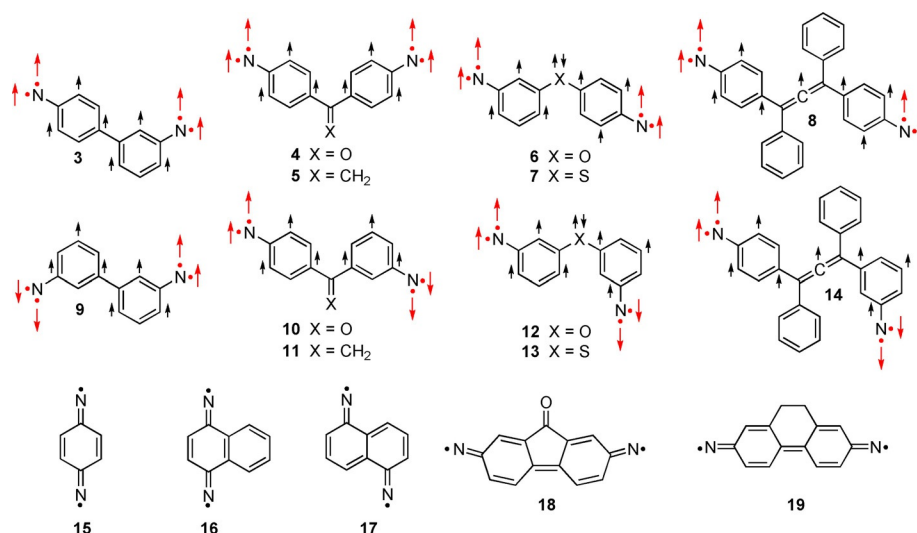


Figure 2. Examples of nondisjoint (3–8), disjoint (9–14) and quinoidal (15–19) dinitrenes.

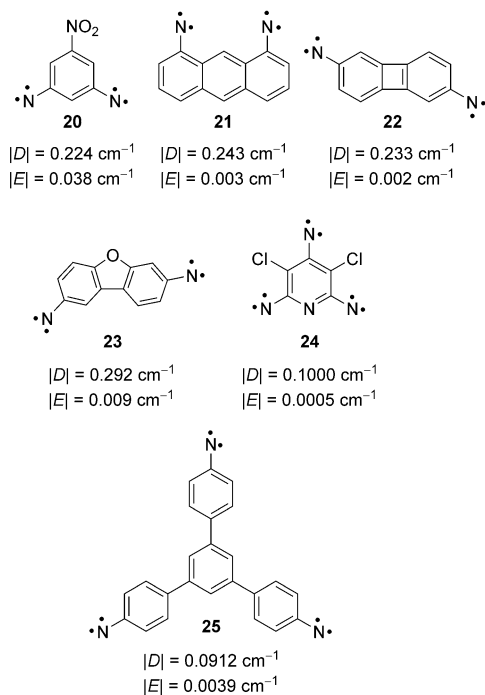


Figure 3. High-spin di- and trinitrenes characterized by EPR spectroscopy.

reliable calculations of  $D$  and  $E$  values at density functional theory (DFT) and ab initio levels of theory.<sup>[21]</sup> The results of these recent studies are discussed here.

## 2. Background

Orbitally nondegenerate magnetic molecules with  $S > 1/2$  are subjected to ZFS, which describes the lifting of the degeneracy of the  $2S+1$  magnetic sublevels  $M_s = S, S-1, \dots, -S$  even in the absence of an external magnetic field. Phenomenologically, this effect is described in the magnetic spin-Hamiltonian of the

Sergei V. Chapyshev received his MSc/1980, PhD/1985, and DSc/2004 degrees from Moscow State University. From 1991 till 2002, he worked as a visiting scientist in Japan, Germany, France, USA and Australia. Since 2007, he collaborates with Prof. Wolfram Sander on investigations of high-spin nitrenes. He is currently a Principal Scientist of the Institute of Problems of Chemical Physics of the Russian Academy of Sciences. He has Awards of the USSR Academy of Sciences and Chemical Society of Japan.



Enrique Méndez Vega received his diploma in chemistry in 2010 from the University of Havana, followed by two years as junior teacher of physical chemistry. Later he joined the group of Prof. Wolfram Sander at Ruhr-University Bochum, obtaining the PhD degree in 2018. He is currently doing postdoctoral work at Sander's group in the field of matrix isolation of carbenes and nitrenes.



Wolfram Sander is Full Professor of Chemistry at the Ruhr-University of Bochum. His research interests in the field of physical organic chemistry focus on the characterization of reactive intermediates, exploring reaction mechanisms, and controlling reactivity by solvent interactions.



general form  $H = SDS$ .<sup>[22]</sup> The traceless  $D$  tensor is referred to as the zero-field tensor and described by two scalar ZFS parameters,  $D$  and  $E$ , characterizing the electronic structure and magnetic properties of high-spin molecules. The conventional notations of the ZFS parameters are  $D = 3/2 D_{zz}$  and  $E = (D_{xx} - D_{yy})/2$ , where  $D_{xx}$ ,  $D_{yy}$ , and  $D_{zz}$  are the eigenvalues of the tensor  $D$ . The "easy axis"  $z$  is defined as  $|D_{zz}| > |D_{xx}|, |D_{yy}|$ . The  $D$  parameter characterizes the energy of the internal anisotropic interactions, and the  $E$  parameter shows magnetic nonequivalence of the perpendicular axes,  $x$  and  $y$ , in the  $D$  tensor.<sup>[22]</sup> Depending on the sign of  $D$ , the magnetization of a molecule can be aligned along an easy axis (negative  $D$ ) or within an easy plane (positive  $D$ ). The larger the negative parameter  $D$  and the total spin of high-spin molecules, the stronger the magnetic properties of the molecules, since the height of an energy barrier between the states with positive and negative magnetic moments with respect to a given axis of magnetization is proportional to  $D$  and  $S^2$ .<sup>[23]</sup> In quintet molecules, the zero-field splittings between the Zeeman energy levels are approximately equal to  $W_{\pm 1} - W_0 = |D|$  and  $W_{\pm 2} - W_{\pm 1} = |3D|$ . In septet molecules, similar splittings plus  $W_{\pm 3} - W_{\pm 2} = |5D|$  are observed. When septet molecules are exposed to the magnetic field, the levels  $W_0$ ,  $W_{\pm 1}$ ,  $W_{\pm 2}$  and  $W_{\pm 3}$  are mixed to form seven distinct energy levels  $W_{-3}$ ,  $W_{-2}$ ,  $W_{-1}$ ,  $W_0$ ,  $W_{+1}$ ,  $W_{+2}$  and  $W_{+3}$ .<sup>[22]</sup>

The first-order EPR spectra of quintet molecules with  $E = 0$  contain four XY and four Z transitions separated by  $D$  and  $2D$ , respectively. The gap between the outer Z<sub>1</sub> and Z<sub>4</sub> transitions is equal to  $6D$ , and the center of the spectrum is located at  $g \approx 2$ .<sup>[22]</sup> Similarly, the first-order EPR spectra of septet molecules with  $E = 0$  contain six XY and six Z transitions separated by  $D$  and  $2D$ , respectively, and the gap between the outer Z<sub>1</sub> and Z<sub>6</sub> transitions equals to  $10D$ .<sup>[22]</sup> These first-order spectra of quintet and septet molecules can be observed by conventional 9.5 GHz EPR spectroscopy only when  $|D| < 0.002 \text{ cm}^{-1}$ . Because quintet and septet nitrenes have  $|D| > 0.09 \text{ cm}^{-1}$ , their 9.5 GHz EPR spectra can reliably be analyzed solely with the aid of modern line-shape EPR spectral simulations<sup>[24]</sup> that are based on an exact numerical matrix diagonalization analysis of the spin Hamiltonian for randomly oriented molecules, as shown in Eq. (1).

$$H = g\beta HS + DS_z^2 - \frac{1}{3}S(S+1)E(S_x^2 - S_y^2) \quad (1)$$

The signs and magnitude of the  $D$  and  $E$  values strongly depend on the molecular structure of quintet and septet nitrenes. Thus, recent EPR studies<sup>[25–27]</sup> have shown that the  $D_Q$  and  $E_Q$  values of quintet dinitrenes, constituted from light atoms, are functions of the vector angles  $\Theta = 2\alpha$  between the nitrene C–N bonds and  $D_t = (\rho_{N_Q}/\rho_{N_T})D_T$  where  $\rho_{N_Q}$  and  $\rho_{N_T}$  are spin densities on the nitrene units of the parent quintet and triplet nitrenes, and  $D_T$  is the  $D$  value of the triplet mononitrene. These dependencies are described by the plot shown in Figure 4 and Eqs. (2) and (3).

$$D_Q = D_t (3 \sin^2 \alpha - 1)/6 \quad (2)$$

$$E_Q = D_t (\cos^2 \alpha)/6 \quad (3)$$

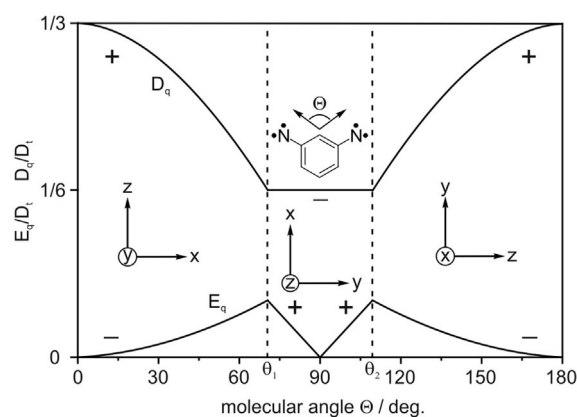


**Figure 4.** Parameters  $D_Q$  and  $E_Q$  and orientations of principal axes  $D_Q$  as function of angle  $\Theta$ . Reprinted from Ref. [27] with permission. Copyright 2008 American Institute of Physics.

In the case of  $C_{2v}$  symmetric septet trinitrenes having two magnetically equivalent nitrene units with  $D_{T1} = D_{T2} = D_T$  and the third nitrene unit with  $D_{T3} = D_T (1 + \lambda)$ , where  $\lambda = (D_{T3} - D_T)/D_T$  the  $D_S$  and  $E_S$  values are described by the plot shown in Figure 5 and Eqs. (4) and (5).<sup>[28]</sup>

$$D_S = -D_t (1 + \lambda/3)/10 \quad (4)$$

$$E_S = D_t [4 \cos^2(\Theta/2) - 1 + \lambda]/30 \quad (5)$$

The number and nature of *exo*-cyclic and *endo*-cyclic atoms in the aromatic rings of quintet and septet nitrenes essentially affect spin-densities on the nitrene units, thus allowing the fine tuning of the magnetic and chemical properties of these compounds. Furthermore, the introduction of heavy atoms in appropriate sites of quintet and septet nitrenes may change the sign and increase several times the  $D$  values of the molecules.<sup>[19,29]</sup> According to theory,<sup>[30,31]</sup> the total tensor  $D^{Tot}$  of high-spin molecules is the sum of two tensors, namely, a first order term  $D^{SS}$  describing the dipolar spin-spin (SS) interactions between unpaired electrons and a second term  $D^{SOC}$  arising

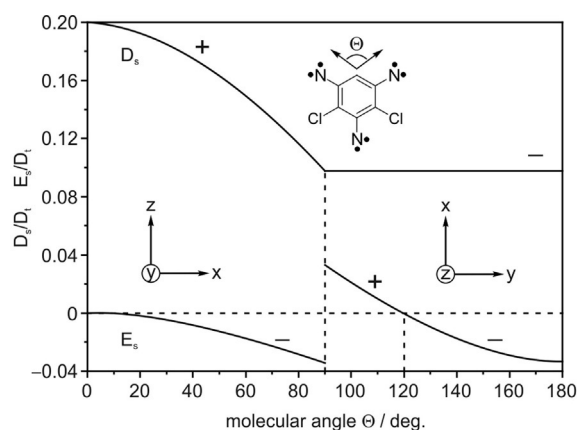


**Figure 5.** Parameters  $D_S$  and  $E_S$  and orientations of principal axes  $D_S$  as function of angle  $\Theta$ . Reprinted from Ref. [28] with permission. Copyright 2008 American Institute of Physics.

from spin-orbit coupling (SOC) as the result of interactions of spins with excited electronic states. In general, the contribution of the SOC-term to  $D^{Tot}$  of high-spin molecules built from light atoms is less than 12%.<sup>[29–31]</sup> However, in case of some bromine-containing quintet and septet nitrenes, the contributions of the SOC-terms to  $D^{Tot}$  are dominant and much surpass the contributions of the  $SS$ -terms.<sup>[19,23]</sup> Nowadays, all effects of the molecular structure on magnetic parameters of high-spin nitrenes are reliably and precisely predicted by DFT and ab initio calculations.<sup>[21]</sup>

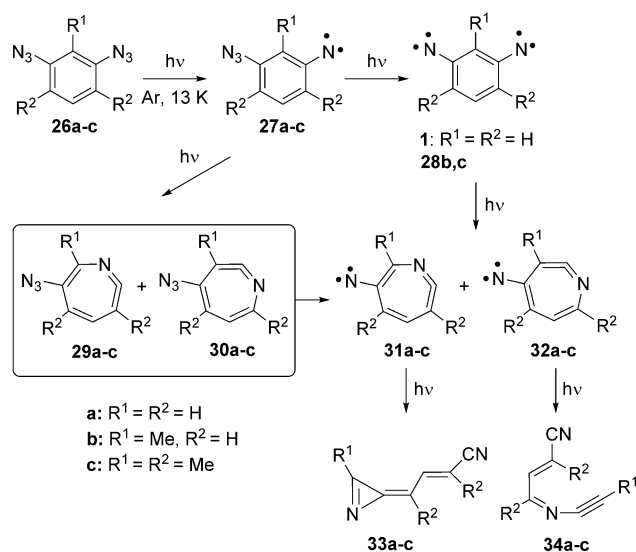
### 3. High-Spin Nitrenes with Benzene Core

#### 3.1. Quintet dinitrenobenzenes

The UV/Vis, IR and EPR studies of the photolysis of diazides **26a–c** in argon matrices are the first comprehensive investigations of quintet dinitrene **1** and its derivatives **28b** and **c** (Scheme 1).<sup>[32,33]</sup>

It was found that dinitrene **1** is photolabile and decomposes to form compounds **33a** and **34a** as the final products.<sup>[32]</sup> The maximum yield of **1** was 34% after 1 min of irradiation of diazide **26a** with light at  $\lambda > 300$  nm. Slightly higher photochemical stability was found for dinitrene **28b**. Its maximum yield reached 44% after 2 min of irradiation of diazide **26b** with light at  $\lambda > 245$  nm. Dinitrene **28c** was rather photostable and was formed in 90% yield after 30 min of irradiation of diazide **26c**. However, on further irradiation, dinitrene **28c** decomposed to form **33c** and **34c**. Despite their photoreactivity, dinitrenes **1**, **27b**, and **27c** displayed intense quintet EPR spectra corresponding to the ZFS parameters listed in Table 1.

A clean UV/Vis spectrum in solid argon was recorded for dinitrene **28b**, displaying five absorption bands with maxima at 307, 326, 395, 418, and 422 nm,<sup>[32]</sup> and in nice agreement with CASSCF and multiconfiguration quasi-degenerate second-order perturbation theory (MCQDPT2) computations.<sup>[34]</sup>



Scheme 1. Photolysis of diazides **26a–c**.

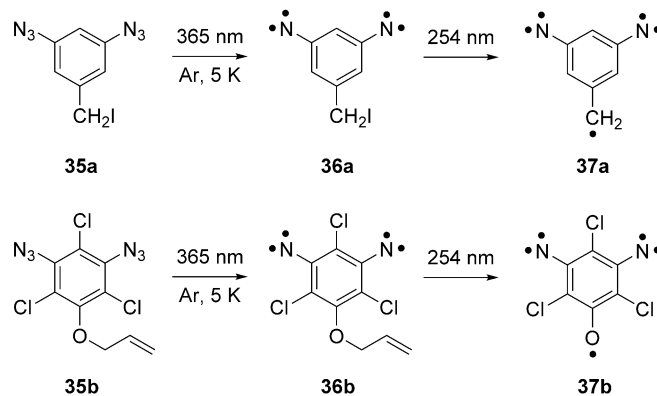
Table 1. ZFS parameters of nitrenes <b>1</b> , <b>28b</b> , and <b>28c</b> . <sup>[33]</sup>		
Nitrene	$ D $ [ $\text{cm}^{-1}$ ]	$ E $ [ $\text{cm}^{-1}$ ]
<b>1</b>	0.202	0.040
<b>28b</b>	0.198	0.034
<b>28c</b>	0.184	0.035

#### 3.2. Sextet dinitreno pentaradicals

Organic molecules bearing a sextet ( $S = 5/2$ ) spin state have received much less attention. Only two sextet pentaradicals were reported, as oligomers of arylmethyl and nitrosyl radical units.<sup>[35–36]</sup> An alternative design involves the ferromagnetic coupling of quintet dinitrenes **28** with an additional C- or O-centered radical, as shown in Scheme 2.

Photolysis of matrix-isolated precursors **35a** and **b** at 5 K with 365 nm light results in the formation of quintet dinitrenes **36a** and **b**, as shown by EPR, IR, and UV/Vis spectroscopy.<sup>[37]</sup> Subsequent irradiation with 254 nm light produces sextet dinitreno radicals **37a** and **b**, according to EPR observations. The sextet **37a** exhibits the ZFS parameters of  $|D| = 0.125 \text{ cm}^{-1}$  and  $|E| = 0.023 \text{ cm}^{-1}$ , whereas for sextet **37b**,  $|D| = 0.088 \text{ cm}^{-1}$  and  $|E| = 0.009 \text{ cm}^{-1}$  were determined. These new sextet organic species exhibit  $D$  values about one order of magnitude larger than previously reported sextet organic pentaradicals, where the spin density was more delocalized into the aromatic system.

#### 3.3. Septet trinitrenobenzenes



Scheme 2. Preparation of quintet **36a,b** and sextet dinitrenes **37a,b**.

Trinitrene **38** is the first septet trinitrene with a benzene core for which the ZFS parameters were determined by means of computer simulations.<sup>[38]</sup> This trinitrene was the major paramagnetic product in the photolysis of 2,4,6-triazidotoluene in cryogenic matrices. In 2-methyltetrahydrofuran (MTHF) glass at 5.5 K trinitrene **38** showed  $|D_5| = 0.0934 \text{ cm}^{-1}$  and  $|E_5| = 0.0015 \text{ cm}^{-1}$ , whereas in solid argon at 4 K, ZFS parameters of  $|D_5| = 0.0938 \text{ cm}^{-1}$  and  $|E_5| = 0.0040 \text{ cm}^{-1}$  were determined. The very small  $E$  value of **38** (Figure 6) in MTHF was explained

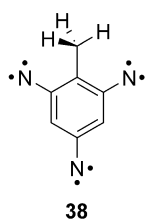
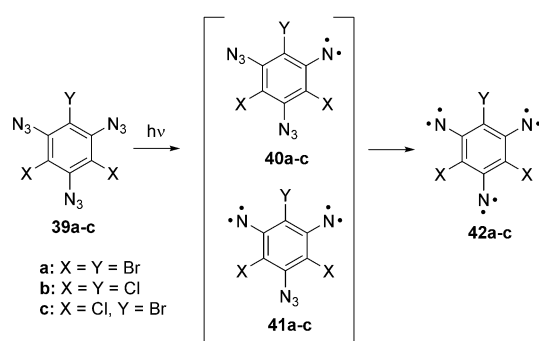


**Figure 6.** The first example of a septet trinitrene with a benzene core.

by re-localization of spin density into the nitrogen atoms due to interaction with surrounding MTHF molecules.

Valuable data on the magnetic and chemical properties of high-spin molecules were obtained by UV/Vis, IR and EPR studies of the photolysis of triazides **39a–c** in various cryogenic matrices (Scheme 3).<sup>[19,39–43]</sup>

The first W-band (94 GHz) EPR spectra (Figure 7) of high-spin nitrenes were recorded for **40a**, **41a**, and **42a**.<sup>[19]</sup> These nitrenes were obtained by photolysis of triazide **39a**. The advantage of W-band EPR spectroscopy on high spin nitrenes is that both the sign and the magnitude of  $D$  can be determined experimentally and compared to theoretical predictions. For septet trinitrene **42a** ZFS values of  $D_5 = -0.203 \text{ cm}^{-1}$  and  $E_5 = 0$  were found, making this molecule the strongest molecular magnet among all known organic septet molecules. Even the metal-



**Scheme 3.** Preparation of trinitrenes **42a–c**.

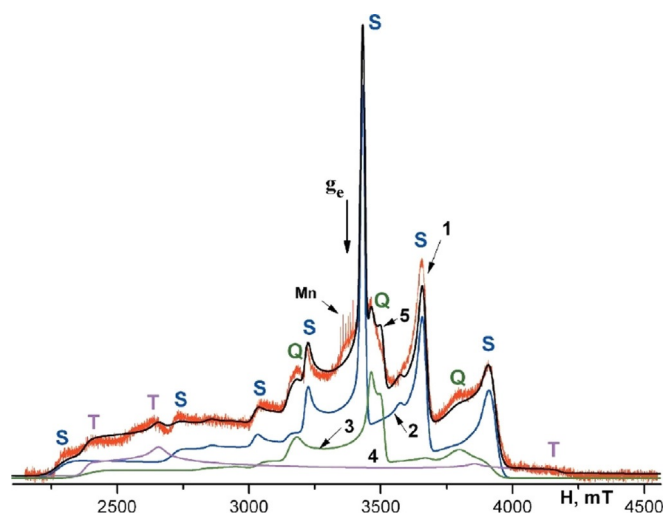


**Figure 7.** Experimental W-band field-swept echo-detected absorption spectrum (red) and simulated spectra of triplet (T) nitrene **40a** (lila), quintet (Q) dinitrene **41a** (green), and septet (S) trinitrene **42a** (blue). Reprinted from Ref. [19] with permission. Copyright 2015 American Institute of Physics.

containing septet molecules MnH and MnF show only  $D_5 = -0.0027$  and  $-0.0083 \text{ cm}^{-1}$ , respectively.<sup>[22]</sup> The unusually large negative  $D_5$  value of **42a** was explained by the effect of heavy bromine atoms adding  $D^{\text{SOC}} \approx -0.11 \text{ cm}^{-1}$  to  $D^{\text{SS}} \approx -0.093 \text{ cm}^{-1}$ . Moreover, for the quintet dinitrene **41a** values of  $D_Q = -0.306 \text{ cm}^{-1}$  and  $E_Q = 0.0137 \text{ cm}^{-1}$ , and for the triplet nitrene **40a** values of  $D_T = 1.369 \text{ cm}^{-1}$  and  $E_T = 0.093 \text{ cm}^{-1}$  were measured. The unexpectedly large negative value of  $D_Q$  for **41a** and the unprecedentedly large  $D_T$  for the triplet phenylnitrene **40a** also result from the effect of the bromine atoms which considerably increase the SOC-terms of these molecules.

The less sensitive X-band (9.5 GHz) EPR studies of the photolysis products of triazides **39a–c** in argon matrices at 15 K revealed that septet trinitrenes **42a–c** are the major paramagnetic products.<sup>[39–42]</sup> Weak EPR signals of transient dinitrenes **41a–c** were detectable only at the initial stages of the reactions, while triplet nitrenes **40a–c** were not observed at all. Trinitrene **42b** showed  $D_5 = -0.0957 \text{ cm}^{-1}$  and  $E_5 = 0$ , and displayed a powder X-band EPR spectrum typical for  $D_{3h}$  symmetric septet molecules with  $|D_5| \approx 0.1 \text{ cm}^{-1}$  and  $E_5 = 0 \text{ cm}^{-1}$  (Figure 8).<sup>[41]</sup> A similar EPR spectrum with a characteristic  $Z_1$  transition at 42 mT was previously reported for trinitrene **2**.<sup>[12]</sup> In the case of **42b**, its  $Z_1$  transition was observed at 18 mT. Analysis of the EPR spectra for **2** and **42b** revealed that the parameter  $D_5$  can be precisely calculated for  $D_{3h}$  symmetric septet molecules using Eq. (6), where  $\nu_0$  is the frequency of microwave irradiation of an EPR spectrometer, and  $H_{Z1}$  is the field position of the  $Z_1$  transition.<sup>[38]</sup>

$$h\nu_0 = |3D_5| + g\beta H_{Z1} \quad (6)$$

For trinitrene **2** the ZFS parameters  $D_5 = -0.092 \text{ cm}^{-1}$  and  $E_5 = 0$  were calculated. Very unusual  $D_5 = 0.1237 \text{ cm}^{-1}$  and  $E_5 = 0.0394 \text{ cm}^{-1}$  were derived from the experimental X-band EPR spectrum of trinitrene **42c**.<sup>[42]</sup> The positive sign of  $D_5$  and unprecedentedly large  $E_5$  of **42c** results from the effect of the bromine atom, considerably increasing the SOC-term and changing the orientation of the easy axis  $Z$  in the molecule. Trinitrene **42c** demonstrates that  $C_{2v}$  symmetrical septet molecules with one heavy atom in the ring have positive  $D_5$  and thus lose the fundamental properties of molecular magnets.

IR studies showed that 365 nm irradiation of triazides **39a, b** in argon matrices at 3 K results in their complete conversion into the corresponding septet trinitrenes **42a, b**. Accordingly, triplet **40a, b**, quintet **41a, b**, or rearranged products were not detected at the end of the photolysis.<sup>[43]</sup> This allowed us recording the first clean IR and UV/Vis spectra for organic septet molecules. The IR spectra of trinitrenes **42a, b** show five signals indicating the formation of highly symmetrical photoproducts and are reasonably well reproduced by M06-2X/aug-cc-pVTZ calculations (Figure 9).

Trinitrene **42b** is chemically rather inert and does not react with  $\text{H}_2$  in solid hydrogen, or with  $\text{O}_2$  in Xe matrices during prolonged annealing at 50 K. Hence, despite bearing three nitrene units and six unpaired electrons, **42b** is even less reactive toward  $\text{O}_2$  than the parent phenylnitrene.<sup>[44]</sup> Trinitrene **42b**

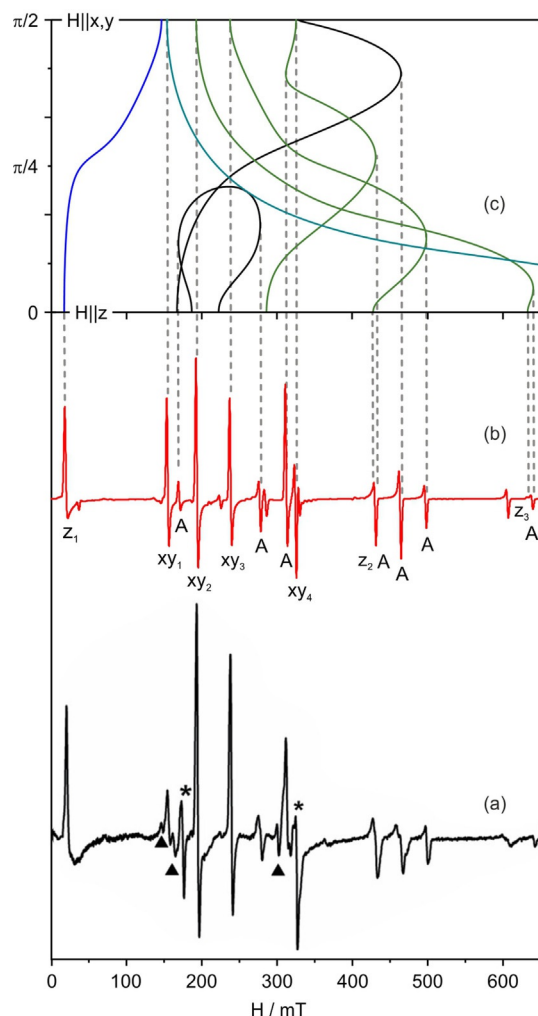


**Figure 8.** Experimental (a), simulated (b) EPR spectra and angular dependencies (c) of trinitrene **42b**. EPR lines marked with (▲) are assigned to dinitrene **41b**, whereas lines marked with (★) arise from impurities in the sapphire rod. Adapted from Ref. [41] with permission. Copyright 2013 American Institute of Physics.

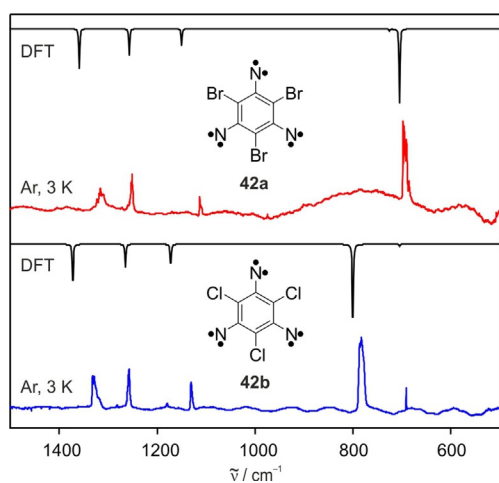


**Figure 9.** Experimental and calculated IR spectra of septet trinitrenes **42a,b**. Adapted from Ref. [43] with permission. Copyright 2019 John Wiley and Sons.

is remarkably persistent in water ice matrices, surviving up to 160 K where the water starts to sublime off.<sup>[43]</sup>

### 3.4. Polynuclear nitrenes

Since polynuclear aromatic systems are promising scaffolds for design of polynitrenes with  $S > 3$ , EPR studies of dinitrene **43** and trinitrene **44**, shown in Figure 10, obtained by photolysis of the corresponding azides in MTHF glass at 5 K, have been carried out.<sup>[45,46]</sup>

According to PBE/DZ/COSMO//B3LYP/6-311+G(d,p) computations, the most stable rotamer of quintet **43** is predicted to have  $D_Q = 0.154 \text{ cm}^{-1}$  and  $E_Q = 0.050 \text{ cm}^{-1}$ , while the lowest energy rotamer of septet **44** gives  $D_S = -0.0904 \text{ cm}^{-1}$  and  $E_S = -0.0102 \text{ cm}^{-1}$ .<sup>[45]</sup> However, simulations using these parameters failed to reproduce the experimental EPR spectra. The successful simulation of the experimental EPR spectrum of **43** was achieved only when very large line-broadening parameters  $\Gamma(E_Q)$  of 1200 MHz (430 G or  $0.04 \text{ cm}^{-1}$ ) along with  $g = 2.003$ ,  $D_Q = 0.154 \text{ cm}^{-1}$  and  $E_Q = 0.050 \text{ cm}^{-1}$  were introduced in the spin Hamiltonian.<sup>[45]</sup> In case of trinitrene **44**, simulations used  $\Gamma(E_Q)$  of 330 MHz ( $0.011 \text{ cm}^{-1}$ ) along with  $g = 2.003$ ,  $D_S = -0.0904 \text{ cm}^{-1}$  and  $E_S = -0.0102 \text{ cm}^{-1}$ .<sup>[46]</sup> These studies show that tetracyclic molecules **43** and **44** exist as mixtures of numerous rotamers possessing different twist angles  $\omega_1$ ,  $\omega_2$  and  $\omega_3$  as well as slightly different  $D$  and  $E$  values. Besides these problems, some of the polynuclear polyazides can undergo undesirable intramolecular reactions. For example, photolysis of tetraazide **45** (Figure 11) in organic glasses at 3 K did not produce the expected nonet tetranitrene. Instead, only a triplet nitrene and two unidentified quintet dinitrenes were observed in the EPR spectra.<sup>[47,48]</sup> It was found that the major products of the reaction are various carbazoles formed in 42% total yield.

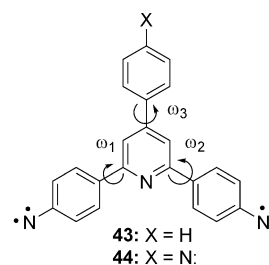


**Figure 10.** Examples of a tetracyclic scaffold that can be used to design high-spin oligonitrenes, such as **43** and **44**.

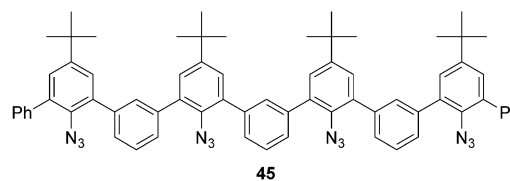


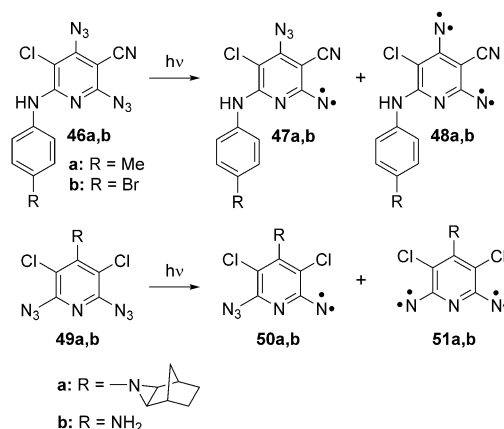
**Figure 11.** Tetraazide **45**, which failed to give the desired tetranitrene due to complex side-reactions during photolysis.

## 4. High-Spin Nitrenes with Pyridine Core

### 4.1. Quintet pyridyldinitrenes

In contrast to diazidobenzenes, diazidopyridines cannot be completely converted into quintet dinitrenes. Thus, photolysis of diazides **46a, b** in MTHF glass at 77 K selectively affords a mixture of triplet nitrenes **47a, b** and quintet dinitrenes **48a, b** in nearly equal amounts (Scheme 4).<sup>[49,50]</sup> Similar photolyses of diazides **49a, b** yields mixtures of triplet **50a, b** and quintet **51a, b**.<sup>[25–27,51–53]</sup>

IR studies in argon matrices show that the ratio **50a** to **51a** at the final stages of the photolysis of **49a** is about 3:7.<sup>[54]</sup> Both **50a** and **51a** do not undergo any undesirable rearrangements and are rather photochemically stable. Dinitrenes **48a, b** display powder X-band EPR spectra characteristic of quintet dinitrenes with  $\theta \approx 120^\circ$  and  $E_Q/D_Q \approx 1:5$ .<sup>[50]</sup> In contrast, dinitrenes **51a, b** exhibit quite unusual EPR spectra corresponding to quintet molecules with  $\theta \approx 115^\circ$  and  $E_Q/D_Q \approx 1/2.9$  in MTHF and  $\approx 1/4$  in argon matrices.<sup>[25–27]</sup> The finding of this new type of quintet dinitrenes stimulated the development of theoretical approaches<sup>[27]</sup> that led to formulation of Eqs. (2) and (3) as well as the plot in Figure 4. The ZFS parameters of dinitrenes **48a, b** and **51a, b** in various matrices are summarized in Table 2. Upon isolation in MTHF glass, dinitrenes **48a, b** and **51a, b** interact with MTHF to form non-bonding molecular complexes of unknown structure. Complexation with MTHF affects the ZFS parameters of **48a, b** and **51a, b** and leads to intense absorption bands with maxima in the 620–640 nm region of their UV/Vis spectra.<sup>[55]</sup>



Scheme 4. Preparation of pyridyldinitrenes **48a,b** and **51a,b**.

Nitrene	Matrix	$ D $ [ $\text{cm}^{-1}$ ]	$ E $ [ $\text{cm}^{-1}$ ]
<b>48a</b> <sup>[46]</sup>	MTHF	0.211	0.043
<b>48b</b> <sup>[46]</sup>	MTHF	0.219	0.044
<b>51a</b> <sup>[26]</sup>	MTHF	0.191	0.0625
<b>51b</b> <sup>[26]</sup>	MTHF	0.202	0.0664
<b>51b</b> <sup>[27]</sup>	Argon	0.210	0.056

Another type of quintet pyridylnitrenes has been obtained in the photolysis of polycrystalline diazide **49b** at 15 K.<sup>[56]</sup> After irradiation with UV light at  $\lambda = 335$  nm for 3 h, the sample displayed relatively weak and broadened EPR lines at 165 and 294 mT, corresponding to bimolecular quintet system **52** with  $g = 2.0023$ ,  $D_Q = 0.251 \text{ cm}^{-1}$  and  $E_Q = -0.030 \text{ cm}^{-1}$  (Figure 12).

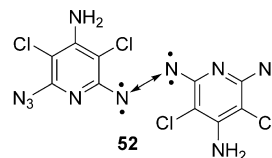
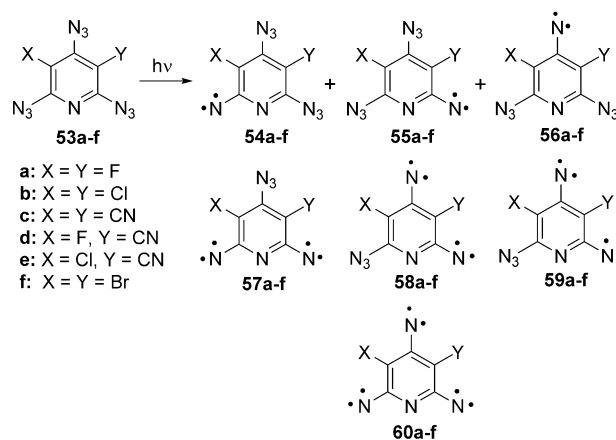


Figure 12. Example of a bimolecular quintet pyridylnitrene, produced from photolysis of polycrystalline diazide **49b**.

### 4.2. Septet pyridyltrinitrenes

Similarly to diazidopyridines, triazidopyridines were photolyzed to give mixtures of various nitrenes. In general, the yields of septet trinitrenes **60b–f** in the photolysis of triazides **53b–f** did not exceed 6% (Scheme 5).<sup>[23,28,57–61]</sup> Only trinitrene **60a** could be obtained by photolysis of **53a** in almost quantitative yields, owing to the small size of the fluorine substituents.<sup>[62]</sup> The total yield of isomeric quintet dinitrenes **57b–f**, **58b–f** and **59b–f** is about 40%, whereas triplet nitrenes **54b–f**, **55b–f** and **56b–f** remain as the major paramagnetic products.<sup>[60–61]</sup> In most cases, the photolysis of nonequivalent  $\alpha$ - and  $\gamma$ -azido groups of triazides **53a–f** occurs selectively to predominantly give triplet nitrenes **54a–f** and quintet dinitrenes **57a–f** as intermediate products.<sup>[23,57–62]</sup> For instance, IR observations show that triplet **54a** and quintet **57a** are selectively formed upon irradiation of triazide **53a** in argon matrices at 4 K.<sup>[62]</sup>

The ZFS parameters of quintet dinitrenes formed in the photolysis of **53a–e** are very similar to those of quintet dinitrenes **48a, b** and **51a, b**. The only exceptions are dinitrenes **57f** and **58f**, containing two heavy bromine atoms in the pyridine ring. Due to the effect of heavy atoms, dinitrene **57f** has  $D_Q =$



Scheme 5. Preparation of pyridyltrinitrenes **60a–f**.

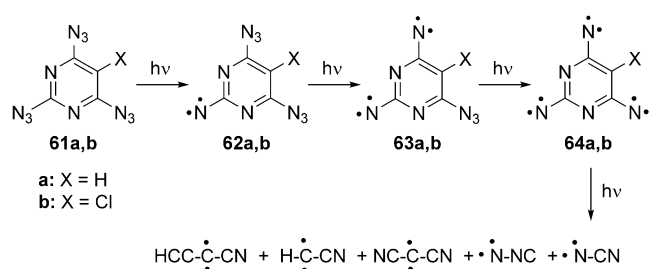
0.289 cm<sup>-1</sup> and  $E_Q=0.0571$  cm<sup>-1</sup>, and its isomer **58 f** shows  $D_Q=0.373$  cm<sup>-1</sup> and  $E_Q=0.0632$  cm<sup>-1</sup>.<sup>[23]</sup> In argon matrices, almost all trinitrenes **60 a–e** show  $D_5 \approx -0.102$  cm<sup>-1</sup> and  $E_5 \approx 0.004$  cm<sup>-1</sup> (Table 3). On comparison with septet trinitrenobenzenes **2**, **38**, and **42 b**, trinitrenes **60 a–e** are somewhat stronger molecular magnets. Trinitrene **60 f** represents a special case.<sup>[23]</sup> Due to the presence of two heavy bromine atoms in the ring, this trinitrene has large positive the  $D_5$  and  $E_5$  values. Analysis of **57 f** shows that  $C_{2v}$  symmetrical septet molecules with two heavy atoms in the ring have positive  $D_5$  and lose the fundamental properties of molecular magnets. Based on the EPR analysis of **60 b**, Eqs. (4) and (5) as well as the plot in Figure 5 indicate dominant SS-terms in the  $D_5$  and  $E_5$  parameters in septet nitrenes.

Attempts to generate septet trinitrenes **60 b, c** by photolysis and  $\gamma$ -radiolysis of polycrystalline triazides **53 b, c** at low temperatures were unsuccessful. Instead, only quintet dinitrenes **57 b, c** and **58 b, c** in a 4:1 ratio were obtained.<sup>[63–68]</sup> These dinitrenes showed remarkable thermal stability, undergoing degradation only on warming the crystals above 230 K.<sup>[62]</sup>

Nitrene	$D_5$ [cm <sup>-1</sup> ]	$E_5$ [cm <sup>-1</sup> ]
<b>60 a</b> <sup>[58]</sup>	-0.1018	0.0037
<b>60 b</b> <sup>[28]</sup>	-0.1019	0.0033
<b>60 c</b> <sup>[59]</sup>	-0.1011	0.0043
<b>60 d</b> <sup>[60]</sup>	-0.1017	0.0042
<b>60 e</b> <sup>[61]</sup>	-0.1021	0.0034
<b>60 f</b> <sup>[23]</sup>	+0.2970	0.0170

## 5. High-Spin Nitrenes with Pyrimidine Core

X-band EPR spectral studies of the photolysis of triazides **61 a, b** in argon matrices at 5 K show the selective formation of triplet nitrenes **62 a, b**, quintet dinitrenes **63 a, b** and septet trinitrenes **64 a, b** (Scheme 6).<sup>[69]</sup> Trinitrene **64 a** is photochemically very unstable and decomposes to triplet nitrenes NCN and NNC as well as triplet carbenes NCCN, HCCN and HCCCN. The latter has never before been generated in a laboratory, but was recently detected by astrophysicists as a component of interstellar matter.<sup>[70]</sup> Photochemical degradation of the chlorine-substituted trinitrene **64 b** yields nitrenes NCN and NNC as well as carbene NCCN. The ZFS parameters of all ni-



Scheme 6. Photolysis of triazides **61 a, b**.

trenopyrimidines formed in the photolysis of **61 a, b** are listed in Table 4. Septet trinitrenes **64 a, b** have large negative  $D_5$  values, exceeding those of septet trinitrenobenzenes and trinitrenopyridines by  $\approx 17$  and  $\approx 10$  %, respectively.

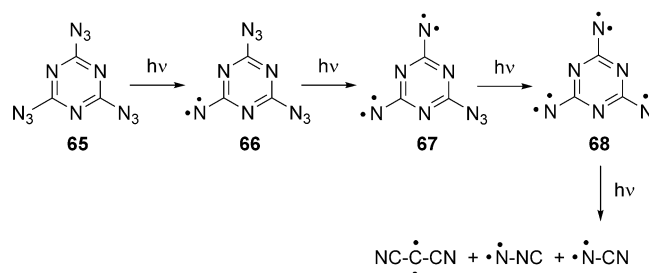
Nitrene	$D$ [cm <sup>-1</sup> ]	$E$ [cm <sup>-1</sup> ]
<b>62 a</b>	1.260	0.0046
<b>62 b</b>	1.170	0.0044
<b>63 a</b>	0.241	0.0540
<b>63 b</b>	0.231	0.0540
<b>64 a</b>	-0.1122	-0.0035
<b>64 b</b>	-0.1119	-0.0058

## 6. High-Spin Nitrenes with s-Triazine Core

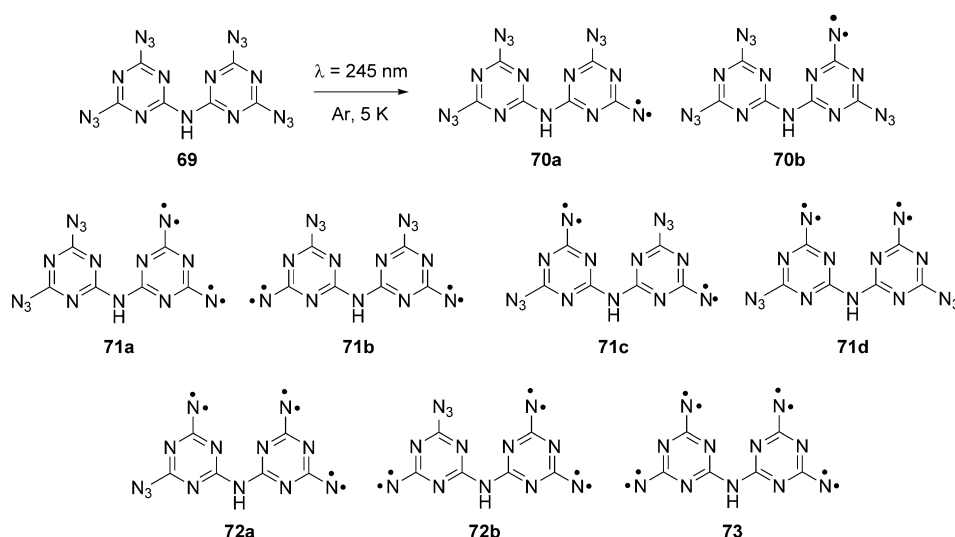
The first attempt to generate high-spin nitrenes with s-triazine core from triazide **65** was reported in 1966.<sup>[71]</sup> It was found that UV irradiation of a single crystal of **65** at 50 K produces the triplet nitrene **66** with  $D_T=1.44$  cm<sup>-1</sup> and  $E_T=0.005$  cm<sup>-1</sup> (Scheme 7). This nitrene displayed a remarkable thermal stability, its EPR signals persisted with only slight loss in intensity for a week at room temperature.

In 1999, the photolysis of **65** was conducted at much lower temperatures (4 K), yielding quintet dinitrene **67**, which was characterized by X-band EPR spectroscopy with  $|D_Q|=0.280$  cm<sup>-1</sup> and  $|E_Q|=0.058$  cm<sup>-1</sup>.<sup>[72]</sup> More recently, the photochemistry of **65** was investigated again, this time in nitrogen matrices at 15 K using UV/Vis, IR and EPR spectroscopy.<sup>[20,73]</sup> It was found that triazide **65** undergoes step-wise photochemical decomposition to subsequently form nitrene **66**, dinitrene **67** and septet trinitrene **68**. The latter showed  $D_5=-0.123$  cm<sup>-1</sup> and  $E_5=0$ .<sup>[20]</sup> This trinitrene was very photolabile and decomposed to form triplet nitrenes NCN and NNC as well as a third unknown triplet product. This unknown product was later identified as carbene NCCN.<sup>[8,69]</sup>

Very recently, the EPR spectral studies of all paramagnetic products formed in the photolysis of tetraazide **69** have been carried out (Scheme 8).<sup>[74]</sup> Photolysis of tetraazide **69** is expected to afford triplet nitrenes **70 a, b**, quintet dinitrenes **71 a–d**, septet trinitrenes **72 a, b** and nonet tetranitrene **73**. According to DFT calculations, all these nitrenes possess high-spin ground states with very large energy gaps (10–40 kcal mol<sup>-1</sup>) between



Scheme 7. Photolysis of triazide **65**.



**Scheme 8.** Photolysis of triazide **69**.

the high- and low-spin states, that should be detectable by EPR spectroscopy. Among these nitrenes, only quintet **71b** and septet **72b** should show negative signs of  $D$  and possess magnetic properties. However, EPR studies of the photolysis of **69** in argon matrices at 5 K showed that only triplet nitrene **70a** with  $D_T = 1.45 \text{ cm}^{-1}$  and  $E_T = 0.0045 \text{ cm}^{-1}$  as well as quintet dinitrene **71a** with  $D_Q = 0.276 \text{ cm}^{-1}$  and  $E_Q = 0.058 \text{ cm}^{-1}$  are obtained. The absence of trinitrenes **72a, b** and tetranitrene **73** after prolonged irradiation might result from the orientation of the aromatic fragments. Only one of the aromatic fragments of the non-planar conformations is properly oriented toward UV light. However, it cannot be excluded that the low photochemical activity of the azido groups in **71a** might be associated with fast transfer of the excitation energy from the diazido-*s*-triazine ring on the neighboring dinitreno-*s*-triazine ring.

## 7. Conclusion and Outlook

The chemistry of high-spin nitrenes is a relatively new research field aimed at designing tunable organic molecules in which spin populations on the Zeeman levels may greatly vary, depending on the external magnetic field and temperature. Despite the fact that first reports on EPR spectra of quintet dinitrene **1** and septet trinitrene **2** were published 50 years ago, the magnetic parameters and molecular structures of these and other derivatives remained unknown for many decades. Only recently, progress in molecular spectroscopy and computational methods opened the way to comprehensive experimental and theoretical studies of these fascinating molecules containing several monovalent nitrogen atoms and large numbers of unpaired electrons. Over a short period of time, dozens of new quintet dinitrenes and septet trinitrenes have been obtained and fully characterized using UV/Vis, IR and EPR spectroscopy. It was observed that most quintet dinitrenes have positive  $D$  parameters and therefore do not possess the funda-

mental properties of molecular magnets. Nevertheless, some of such molecules, for example, dinitrene **41a** with  $D_Q = -0.306 \text{ cm}^{-1}$  and dinitrene **71b** with  $D_Q = -0.247 \text{ cm}^{-1}$ , are true molecular magnets owing to their specific molecular structures. On the other hand, most septet trinitrenes show large negative  $D_S$  parameters exceeding by several orders the  $D_S$  values of metal-containing septet molecules such as MnH and MnF. The magnitude of  $D_S$  strongly depends on the molecular structure of the septet nitrenes. Among such nitrenes with small SOC-terms, the largest  $D_S$  of  $-0.123 \text{ cm}^{-1}$  was found for trinitrene **68**. However, this trinitrene is very photolabile which hampers potential applications. Septet trinitrenes **64a** and **b** based on pyrimidine cores exhibit  $D_S \approx -0.112 \text{ cm}^{-1}$ , but are also photoreactive. Although the pyridine-containing septet trinitrenes **60a–e** are photostable and show  $D_S \approx -0.102 \text{ cm}^{-1}$ , only trinitrene **60a** can be generated in high yields by photolysis of the corresponding triazide. Fortunately, the best combination of all necessary parameters such as high yields, high photochemical and thermal stability, chemical inertness, and large negative  $D_S$ , has been revealed for septet trinitrenobenzenes **42a** and **b**. Of these compounds, trinitrene **42b** with a relatively small SOC-term shows  $D_S = -0.0957 \text{ cm}^{-1}$ . In contrast, trinitrene **42b**, possessing a large SOC-term due to the three bromine atoms, exhibits the largest magnetic anisotropy ( $D_S = -0.203 \text{ cm}^{-1}$ ) among all organic septet molecules. The studies of trinitrenes **42c** and **60f**, with positive  $D_S$ , also reveal that trinitrenes lose magnetism on introduction of one or two heavy atoms in the six-membered aromatic ring.

Another key factor for the design of effective molecular magnets is that the high-spin ground state must be separated from the low-spin excited states by an energy gap significantly greater than the thermal energy at ambient temperature (RT  $\approx 0.6 \text{ kcal mol}^{-1}$ ). According to CASSCF and DFT calculations, di- and trinitrenobenzenes typically have energy gaps in the range of 5–10  $\text{kcal mol}^{-1}$ .<sup>[16,75]</sup> These high-spin nitrenes are thermally stable towards rearrangements, but exhibit high bimo-

lecular reactivity in solution. However, in appropriate solid phases (e.g. in host crystals of nitroaromatics) some oligonitrenes can live for years at room temperature without changes.<sup>[76]</sup> Therefore, the search for the optimum solid phase for long-time conservation of high-spin nitrenes at room temperature is of key importance for the design of new magnetic materials based on high-spin nitrenes. On the other hand, the nature of the aromatic core in the starting polyazides is also very important. Although high-spin nitrenes formed from azidoazines have the highest spin-populations on the nitrene units and the largest  $D^{SS}$ , the photochemical generation of these nitrenes in crystals is rather problematic,<sup>[63–68,71–72]</sup> presumably due to the effect of the nitrogen lone electron pair on the N–N<sub>2</sub> dissociation in the excited states.<sup>[69]</sup> By contrast, arylazides do not have *endo*-cyclic nitrogen atoms and readily form high-spin nitrenes in almost quantitative yields during photolysis. These arylazides can also bear heavy atoms on the aromatic core and form nitrenes with large  $D^{SOC}$  and negative magnetic anisotropy.

A number of multi-spin molecular systems are currently considered as promising materials for the design of quantum computers.<sup>[77]</sup> Most studies focus on inorganic molecular magnets, for example,  $[\text{GdP}_5\text{W}_{30}\text{O}_{110}]^{12-}$  with  $S=7/2$  and  $D=-0.124\text{ cm}^{-1}$ , representing an eight-level quantum qudit composed of three qubits.<sup>[78]</sup> In diamagnetic  $\text{YW}_{30}$  crystals doped with  $\text{GdW}_{30}$ , seven allowed EPR transitions of  $\text{GdW}_{30}$  can coherently be manipulated by using 9.8 GHz microwave pulses. To achieve the high purity of the signals and large coherence time  $T_2$  for spin states, all operations are performed at cryogenic temperatures. In principle, a similar approach could be envisioned using high-spin nitrenes fixed in an appropriate solid phase. Recent studies have shown that matrix-isolated septet trinitrene **60a** has 17 allowed EPR transitions and formally represents a seven-level quantum qudit composed of 17 qubits.<sup>[58]</sup> The preparation of quantum qudits from nitrenes would be simpler and less expensive than the design of lanthanide complexes with a priori unpredictable magnetic properties. The recent progress in investigations of high-spin nitrenes opens the way to practical application of these magnetic species in molecular electronics and spintronics.

## Acknowledgements

This work was funded by the Russian State Program AAAA-A19-119070790003-7 and the Deutsche Forschungsgemeinschaft (DFG, German Research Foundation) under Germany's Excellence Strategy–EXC-2033–Projektnummer 390677874. We thank Stefan Henkel for assistance with EPR simulations. Open access funding enabled and organized by Projekt DEAL.

## Conflict of interest

The authors declare no conflict of interest.

**Keywords:** EPR spectroscopy · matrix isolation · magnetism · nitrenes · radicals

- [1] W. Lwowski, *Nitrenes*, Wiley, New York, 1970.
- [2] C. Wenstrup, *Reactive Molecules: The Neutral Reactive Intermediates in Organic Chemistry*, Wiley, New York, 1984.
- [3] E. F. V. Scriven, *Azides and Nitrenes, Reactivity and Utility*, Academic Press, New York, 1984.
- [4] C. Wenstrup, *Angew. Chem. Int. Ed.* **2018**, *57*, 11508–11521; *Angew. Chem.* **2018**, *130*, 11680–11693.
- [5] P. M. Lahti, M. Minato, C. Ling, *Mol. Cryst. Liq. Cryst.* **1995**, *271*, 147–154.
- [6] P. M. Lahti, *Magnetic Properties of Organic Materials*, Marcel Dekker, New York 1999.
- [7] S. V. Chapyshev, *Russ. Chem. Bull.* **2011**, *60*, 1274–1285.
- [8] S. V. Chapyshev, *Molecules* **2015**, *20*, 19142–19171.
- [9] D. E. Falvey, A. D. Gudmundsdottir, in *Wiley Series of Reactive Intermediates in Chemistry and Biology* (Ed.: S. E. Rokita), Wiley, Hoboken, **2013**.
- [10] G. Smolinsky, E. Wasserman, Y. A. Yager, *J. Am. Chem. Soc.* **1962**, *84*, 3220–3221.
- [11] E. Wasserman, R. W. Murray, W. A. Yager, A. M. Trozzolo, G. Smolinsky, *J. Am. Chem. Soc.* **1967**, *89*, 5076–5078.
- [12] E. Wasserman, K. Schueller, W. A. Yager, *Chem. Phys. Lett.* **1968**, *2*, 259–260.
- [13] T. A. Fukuzawa, K. Sato, A. S. Ichimura, T. Kinoshita, T. Takui, K. Itoh, P. M. Lahti, *Mol. Cryst. Liq. Cryst.* **1996**, *278*, 253–260.
- [14] R. S. Kalgutkar, P. M. Lahti, *Tetrahedron Lett.* **2003**, *44*, 2625–2628.
- [15] R. S. Kalgutkar, P. M. Lahti, *J. Am. Chem. Soc.* **1997**, *119*, 4771–4772.
- [16] S. V. Chapyshev, R. Walton, J. A. Sanborn, P. M. Lahti, *J. Am. Chem. Soc.* **2000**, *122*, 1580–1588.
- [17] N. Oda, T. Nakai, K. Sato, D. Shiomi, M. Kozaki, K. Okada, T. Takui, *Synth. Met.* **2001**, *121*, 1840–1841.
- [18] N. Oda, T. Nakai, K. Sato, D. Shiomi, M. Kozaki, K. Okada, T. Takui, *Mol. Cryst. Liq. Cryst.* **2002**, *376*, 501–506.
- [19] A. Akimov, A. Masitov, D. Korchagin, S. Chapyshev, E. Y. Misochko, A. Savitsky, *J. Chem. Phys.* **2015**, *143*, 084313.
- [20] T. Sato, A. Narazaki, Y. Kawaguchi, H. Niino, G. Bucher, D. Grote, J. J. Wolff, H. H. Wenk, W. Sander, *J. Am. Chem. Soc.* **2004**, *126*, 7846–7852.
- [21] F. Neese, *Wiley Interdiscip. Rev.: Comput. Mol. Sci.* **2012**, *2*, 73–78.
- [22] W. Weltner, Jr., *Magnetic Atoms and Molecules*, Dover, New York, **1989**.
- [23] E. Y. Misochko, A. V. Akimov, A. A. Masitov, D. V. Korchagin, I. K. Yakushchenko, S. V. Chapyshev, *J. Chem. Phys.* **2012**, *137*, 064308.
- [24] S. Stoll, A. J. Schweiger, *J. Magn. Reson.* **2006**, *178*, 42–55.
- [25] S. V. Chapyshev, *Russ. Chem. Bull.* **2006**, *55*, 1593–1597.
- [26] S. V. Chapyshev, P. M. Lahti, *J. Phys. Org. Chem.* **2006**, *19*, 637–641.
- [27] E. Y. Misochko, A. V. Akimov, S. V. Chapyshev, *J. Chem. Phys.* **2008**, *128*, 124504.
- [28] E. Y. Misochko, A. V. Akimov, S. V. Chapyshev, *J. Chem. Phys.* **2008**, *129*, 174510.
- [29] D. V. Korchagin, A. V. Akimov, A. Savitsky, S. V. Chapyshev, S. M. Aldoshin, E. Y. Misochko, *J. Phys. Chem. A* **2018**, *122*, 8931–8937.
- [30] K. Sugisaki, K. Toyota, K. Sato, D. Shiomi, M. Kitagawa, T. Takui, *ChemPhysChem* **2010**, *11*, 3146–3151.
- [31] K. Sugisaki, K. Toyota, K. Sato, D. Shiomi, M. Kitagawa, T. Takui, *Phys. Chem. Chem. Phys.* **2014**, *16*, 9171–9181.
- [32] S. V. Chapyshev, H. Tomioka, *Bull. Chem. Soc. Jpn.* **2003**, *76*, 2075–2089.
- [33] S. V. Chapyshev, *Russ. Chem. Bull.* **2006**, *55*, 1126–1131.
- [34] K. Sugisaki, K. Toyota, K. Sato, D. Shiomi, T. Takui, *Angew. Chem. Int. Ed.* **2006**, *45*, 2257–2260; *Angew. Chem.* **2006**, *118*, 2315–2318.
- [35] A. Rajca, S. Rajca, S. R. Desai, *J. Am. Chem. Soc.* **1995**, *117*, 806–816.
- [36] J. Fujita, Y. Matsuoka, K. Matsuo, M. Tanaka, T. Akita, N. Koga, H. Iwamura, *Chem. Commun.* **1997**, *24*, 2393.
- [37] J. Mieres-Mieres-Pérez, S. Henkel, E. Mendez-Vega, T. Schleif, T. Lohmiller, A. Savitsky, W. Sander, *J. Phys. Org. Chem.* **2017**, *30*, e3621.
- [38] S. V. Chapyshev, E. Y. Misochko, A. V. Akimov, V. G. Dorokhov, P. Neuhaus, D. Grote, W. Sander, *J. Org. Chem.* **2009**, *74*, 7238–7244.
- [39] E. Y. Misochko, A. V. Akimov, A. A. Masitov, D. V. Korchagin, I. K. Yakushchenko, S. V. Chapyshev, *Russ. Chem. Bull.* **2015**, *64*, 87–91.
- [40] E. Y. Misochko, A. V. Akimov, A. A. Masitov, D. V. Korchagin, S. V. Chapyshev, *Russ. Chem. Bull.* **2012**, *61*, 2218–2224.

- [41] E. Y. Misochko, A. V. Akimov, A. A. Masitov, D. V. Korchagin, S. M. Aldoshin, S. V. Chapyshev, *J. Chem. Phys.* **2013**, *138*, 204317.
- [42] E. Y. Misochko, A. A. Masitov, A. V. Akimov, D. V. Korchagin, S. V. Chapyshev, *J. Phys. Chem. A* **2015**, *119*, 2413–2419.
- [43] E. Mendez-Vega, J. Mieres-Perez, S. V. Chapyshev, W. Sander, *Angew. Chem. Int. Ed.* **2019**, *58*, 12994–12998; *Angew. Chem.* **2019**, *131*, 13128–13132.
- [44] J. Mieres-Perez, E. Mendez-Vega, K. Velappan, W. Sander, *J. Org. Chem.* **2015**, *80*, 11926–11931.
- [45] S. V. Chapyshev, D. V. Korchagin, M. F. Budyka, T. N. Gavriushova, P. Neuhaus, W. Sander, *J. Phys. Chem. A* **2011**, *115*, 8419–8425.
- [46] S. V. Chapyshev, D. V. Korchagin, M. F. Budyka, T. N. Gavriushova, P. Neuhaus, W. Sander, *ChemPhysChem* **2012**, *13*, 2721–2728.
- [47] H. Oka, Y. Miura, Y. Teki, *Mol. Cryst. Liq. Cryst.* **1999**, *334*, 41–48.
- [48] Y. Miura, H. Oka, Y. Teki, *Bull. Chem. Soc. Jpn.* **2001**, *74*, 385–386.
- [49] S. V. Chapyshev, R. Walton, P. M. Lahti, *Mendeleev Commun.* **2000**, *10*, 7–9.
- [50] S. V. Chapyshev, R. Walton, P. R. Serwinski, P. M. Lahti, *J. Phys. Chem. A* **2004**, *108*, 6643–6649.
- [51] S. V. Chapyshev, R. Walton, P. M. Lahti, *Mendeleev Commun.* **2000**, *10*, 114–115.
- [52] S. V. Chapyshev, P. R. Serwinski, *Mendeleev Commun.* **2001**, *11*, 92–94.
- [53] E. Y. Misochko, A. V. Akimov, V. F. Lavitskii, S. V. Chapyshev, *Russ. Chem. Bull.* **2007**, *56*, 2364–2369.
- [54] S. V. Chapyshev, A. Kuhn, M. W. Wong, C. Wentrup, *J. Am. Chem. Soc.* **2000**, *122*, 1572–1579.
- [55] S. V. Chapyshev, *Mendeleev Commun.* **2002**, *12*, 168–170.
- [56] S. V. Chapyshev, V. F. Lavitskii, A. V. Akimov, E. Y. Misochko, A. V. Shastin, D. V. Korchagin, G. V. Shilov, S. M. Aldoshin, *Russ. Chem. Bull.* **2008**, *57*, 524–531.
- [57] S. V. Chapyshev, R. Walton, P. M. Lahti, *Mendeleev Commun.* **2000**, *10*, 187–188.
- [58] S. V. Chapyshev, D. Grote, C. Finke, W. Sander, *J. Org. Chem.* **2008**, *73*, 7045–7051.
- [59] S. V. Chapyshev, P. Neuhaus, D. Grote, W. Sander, *J. Phys. Org. Chem.* **2010**, *23*, 340–346.
- [60] S. V. Chapyshev, D. V. Korchagin, D. Grote, W. Sander, *Magn. Reson. Chem.* **2019**, *57*, 472–478.
- [61] S. V. Chapyshev, D. V. Korchagin, P. Neuhaus, W. Sander, *Beilstein J. Org. Chem.* **2013**, *9*, 733–741.
- [62] C. Finke, D. Grote, R. W. Seidel, S. V. Chapyshev, W. Sander, *J. Phys. Org. Chem.* **2012**, *25*, 486–492.
- [63] S. I. Kuzina, A. I. Mikhailov, S. V. Chapyshev, *High Energy Chem.* **2007**, *41*, 245–250.
- [64] S. I. Kuzina, A. I. Mikhailov, S. V. Chapyshev, *Doklady Phys. Chem.* **2007**, *412*, 34–37.
- [65] S. I. Kuzina, S. V. Tokarev, D. V. Korchagin, G. A. Kolpakov, D. V. Khudyakov, S. V. Chapyshev, A. I. Mikhailov, V. A. Nadtochenko, S. M. Aldoshin, *Russ. Chem. Bull.* **2013**, *62*, 255–264.
- [66] S. I. Kuzina, A. I. Mikhailov, S. V. Chapyshev, D. V. Korchagin, G. V. Shilov, S. M. Aldoshin, *Russ. J. Phys. Chem. A* **2008**, *82*, 1870–1877.
- [67] S. I. Kuzina, A. I. Mikhailov, S. V. Chapyshev, D. V. Korchagin, G. V. Shilov, S. M. Aldoshin, *Mendeleev Commun.* **2007**, *17*, 207–208.
- [68] S. I. Kuzina, D. V. Korchagin, G. V. Shilov, S. V. Chapyshev, A. I. Mikhailov, S. M. Aldoshin, *Doklady Phys. Chem.* **2008**, *418*, 7–12.
- [69] S. V. Chapyshev, E. N. Ushakov, P. Neuhaus, W. Sander, *J. Org. Chem.* **2014**, *79*, 6047–6053.
- [70] J. Cernicharo, M. Guelin, J. R. Pardo, *Astrophys. J.* **2004**, *615*, L145–L148.
- [71] R. M. Moriarty, M. Rahman, G. J. King, *J. Am. Chem. Soc.* **1966**, *88*, 842–843.
- [72] T. Nakai, K. Sato, D. Shiomi, T. Takui, K. Itoh, M. Kozaki, K. Okada, *Mol. Cryst. Liq. Cryst.* **1999**, *334*, 157–166.
- [73] T. Sato, A. Narazaki, Y. Kawaguchi, H. Niino, G. Bucher, *Angew. Chem. Int. Ed.* **2003**, *42*, 5206–5209; *Angew. Chem.* **2003**, *115*, 5364–5367.
- [74] S. V. Chapyshev, D. V. Korchagin, P. Costa, W. Sander, *J. Photochem. Photobiol. A* **2019**, *377*, 207–213.
- [75] A. S. Ichimura, P. M. Lahti, *Mol. Cryst. Liq. Cryst.* **1993**, *233*, 34–40.
- [76] A. S. Ichimura, K. Sato, T. Kinoshita, T. Takui, K. Itoh, P. M. Lahti, *Mol. Cryst. Liq. Cryst.* **1995**, *272*, 57–66.
- [77] A. Gaita-Ariño, F. Luis, S. Hill, E. Coronado, *Nat. Chem.* **2019**, *11*, 301–309.
- [78] M. D. Jenkins, Y. Duan, B. Diosdado, J. J. Garcia-Ripoll, A. Gaita-Arino, C. Gimenez-Saiz, P. J. Alonso, E. Coronado, F. Luis, *Phys. Rev. B* **2017**, *95*, 064423.

---

Manuscript received: May 5, 2020

Revised manuscript received: June 23, 2020

Accepted manuscript online: June 24, 2020

Version of record online: November 5, 2020